Research Square

Preprints are preliminary reports that have not undergone peer review.
They should not be considered conclusive, used to inform clinical practice,
or referenced by the media as validated information.

Analyzing Future Rainfall Variations Over Southern Malay Peninsula Based On CORDEX-SEA Dataset

Xiaosheng Qin (xsqin@ntu.edu.sg)
Nanyang Technological University https://orcid.org/0000-0003-3187-7561
Chao Dai
Nanyang Technological University
Lilingjun Liu
Nanyang Technological University

Research Article

Keywords: rainfall variability, Peninsular Malaysia, Singapore, APHRODITE, CORDEX

Posted Date: July 20th, 2021

DOI: https://doi.org/10.21203/rs.3.rs-681108/v1

License: This work is licensed under a Creative Commons Attribution 4.0 International License.
Read Full License

Analyzing Future Rainfall Variations Over Southern Malay Peninsula Based on CORDEX-SEA Dataset

Xiaosheng Qin*, Chao Dai, Lilingjun Liu

School of Civil and Environmental Engineering, Nanyang Technological University, 50 Nanyang Avenue, Singapore 639798

*Corresponding author: Dr. Qin Xiaosheng, School of Civil and Environmental Engineering, Nanyang Technological University, 50 Nanyang Avenue, Singapore 639798; Tel: +65-67905288; Fax: +65-67921650; E-mail: xsqin@ntu.edu.sg; ORCID: 0000-0003-3187-7561

Abstract

Gridded rainfall datasets based on various data sources and techniques have emerged to help describe the spatiotemporal features of rainfall patterns over large areas and have gained popularity in many regional/global climatic analyses. This study explored future variations of rainfall characteristics over peninsula Malaysia and Singapore region based on rainfall indices of PRCPTOT, Rx1day, Rx5day, R95pTOT, R1mm, and R20mm, under 9 CORDEX-SEA RCM datasets with RCP8.5 emission scenario. A monthly quantile delta mapping method (MQDM) was adopted for bias-correction of the RCM modelled data. It was indicated that all the studied rainfall indices have long-term variations both temporally and spatially. Generally, the further the future, the higher the variability and uncertainty of indices. For the study region, the relative increments of the medians from RCM models averaged over all climatic zones in the far future are 40.3%, 25.9%, and 4.7% for Rx1day, Rx5day and R95pTOT, respectively. The annual rainfall amount (PRCPTOT) in the long run would likely increase mainly in the northeast coastal zone and drop in most of other areas over the peninsula, with the median being -5.9% averaged over all zones. The frequency of wet days (R1mm) would generally drop over the whole peninsula, with the median averaged over all zones being -6.8% in the far future. The frequency of heavy rains (R20mm) would overall decrease (by -3.4% in average in the far future) but might still notably increase in the northeast zone (NE) at both annual and southwest monsoon. The extreme condition implied from various RCM models would be more alarming. The study result would be useful in revealing the essential spatiotemporal variations of rainfall over the peninsula from short- to long-term futures and supporting large-scale flood risk assessment and adaptation planning.

Key words: rainfall variability; Peninsular Malaysia; Singapore; APHRODITE; CORDEX

1. INTRODUCTION

Analysis of climate variability at a regional scale is important for the understanding of regional hydrological features and planning of water resources at large-scale river basins. This is especially true for Southeast Asia (SEA), where the economic conditions, resources availability, and adaptive capability to climate extremes are highly diversified. The southern part of Malay Peninsula, located at the southernmost Asian continent, is a relatively small portion of SEA region characterized by tropical climate, two monsoonal seasons, high geographical differences, and vulnerability to climate change (Cavendish Square Publishing, 2007). This region consists of mainly western Malaysia and Singapore and is encircled by the southwestern section of Thailand, the Malacca Strait, the Singapore Strait, and the South China Sea. Over the past decades, this region has undergone a rapid economic development but is also facing challenges of extreme weather events and water supply issues (Hai et al., 2017; Chow, 2017). Analysis of rainfall patterns over this region would greatly enhance the understanding of the hydrological trends and variability and the design of responsive actions of regional flooding, drought, and drainage system design.

In recent decades, gridded rainfall datasets based on various data sources and techniques have emerged to help describe the spatiotemporal features of rainfall patterns over large areas and have gained popularity in many regional/global climatic analyses (Donat et al., 2014). A detailed review of global precipitation datasets has been provided by Sun et al. (2017). For future climate

change studies, the Coordinated Regional Climate Downscaling Experiment (CORDEX) datasets have been widely used for grid-level based impact study from climate change. The CORDEX has been a multinational effort under the World Climate Research Programme (WCRP) framework in running regional climate models (RCMs) through standardized experiments, targeting at offering high-resolution climate projections for the world (Giorgi et al., 2009; Evans, 2011). In recent years, there have been a few research efforts devoted in using CORDEX or RCM products for climate change impact assessment in the context of SEA. For examples, Ngai et al. (2017) used results from four RCMs and the corresponding global circulation models (GCMs) from CORDEX-EA datasets to analyze the long-term trends of daily precipitation and temperature over the entire Southeast Asia. The trend preserving quantile mapping (QM) method was used in this study and proved to have capability of greatly improving the biases from large-scale model outputs. Tangang et al. (2019) presented changes of rainfall over Thailand in various future windows using RCP4.5 and RCP8.5 based on seven RCM outputs from CORDEX simulations. Tangang et al. (2020) has given an important examination on the projected variations of rainfall in SEA based on multiple model simulations from Southeast Asia Regional Climate Downscaling (SEACLID)/CORDEX-SEA. Supari et al. (2020) investigated projections of four precipitation extremes (including total rainfall amount, consecutive dry days, frequency of heavy rainfall based on 50 mm, and daily maximum rainfall) over both annual and seasonal scales over the large SEA domain based on eight CORDE-SEA datasets with both RCP4.5 and RCP8.5 emission scenarios.

In the context of the southern part of Malay Peninsula, there are a few related studies reported recently. For examples, Amin et al. (2017) studied the water balance and flood condition in the 21st century over Muda and Dungun watersheds over Peninsula Malaysia using a coupled climate and hydrology model under 15 GCM-driven RCM downscaled scenarios. Tan et al. (2020) studied the hydrometeorological droughts over the Kelantan River Basin, Malaysia, based on CORDEX-SEA projections and a distributed hydrological model. Ngai et al. (2020a) used a non-hydrostatic RCM (NHRCM) to simulate future rainfall over Malaysia under RCP8.5 scenario based on six extreme rainfall indices. Ngai et al. (2020b) adopted a quantile mapping (QM) method to bias-correct rainfall data from seven CORDEX rainfall products datasets and project future rainfall patterns over Malaysia based on three rainfall indices related to rain-day frequency, intensity, and 90th percentile of rain-day precipitation amount.

Generally, the previous studies are valuable in assessing the variations of rainfall patterns under climate change over SEA or entire Malaysia. It is also necessary to give a more detailed examination on the rainfall patterns over the southern part of Malay Peninsula (including Peninsula Malaysia and Singapore regions), considering the availability of more updated CORDEX-SEA datasets and also the importance of having a more holistic view on the uncertainty of rainfall variability from ensembled RCM outputs. Furthermore, it would be value-added effort to explore more effective bias-correction approach for this study region to improve the reliability of future projections. Thus, as an extension to the work of Ngai et al. (2020b), this study aims at exploring future variations of rainfall characteristics from the angle of rainfall

amount, frequency, and extremes using six standard rainfall indices, based on 9 CORDEX-SEA RCM datasets with RCP8.5 emission scenario. A monthly quantile delta mapping approach will be adopted for bias-correction of the RCM modelled data. The future analysis will be based on climatic zones over the peninsula defined by Wong et al. (2016), for the benefit of better quantification of spatial rainfall extreme variations and adaptation planning of water-induced crisis in face of future climate change in the study region.

2. STUDY AREA, DATA AND METHOD

Study Area and Data

The study area will primarily focus on the southern part of the Malay Peninsula (as shown in Figure 1), consisting of Peninsular Malaysia (west Malaysia) and the city state of Singapore (i.e. 100.0-104.5E and 1.0-7.0N), with a total land area over 132 thousand km^2. The southern Malay Peninsula topography is featured by highlands, coastal regions, and floodplains, with the major mountain range (i.e. Titiwangsa Range) extending from north to south and separating west and east coast regions. As this area is close to the equator, its climate is mostly hot and humid throughout the year. The average annual rainfall is around 2,400 mm and temperature ranges from 25 to 32^{o}C (Wong et al., 2016; Ahmad et al., 2017). Most of the peninsula is affected by two monsoons, including southwest monsoon (from May to September) and northeast one (from November to March), with Singapore location having slightly delayed month in each monsoon (Suhaila et al., 2010; Li et al., 2019). The climate of the study area is strongly affected by the

monsoon winds and also the global effects (like EL Niño-Southern Oscillation), making it susceptible to increased risks of flooding and droughts under climate change conditions (Tangang et al., 2017; Richard and Walsh, 2018). For the convenience of spatial description, we adopt the eight climatic zones delineated by Wong et al. (2016), to cover the study area and highlight climate change impacts. Figure 1 also shows the boundaries of all zones.

Place Figure 1 Here

The historical data (from 1970 to 2005) used for this study are based on Asian Precipitation-Highly-Resolved Observational Data Integration toward Evaluation of Water Resources (APHRODITE) rainfall dataset (APHRO_MA V1101) at 0.25 degree resolution (http://aphrodite.st.hirosaki-u.ac.jp/products.html). The dataset was based on a wide range of gauge rainfall data and interpolated over a large domain (Yatagai et al. 2012). For future climate data, we have selected 9 rainfall datasets with scenario RCP8.5 from the Coordinated Regional Climate Downscaling Experiment for Southeast Asia (CORDEX-SEA), with details being provided in Table 1 (Giorgi et al, 2012; Kjellström et al., 2014; Ngo-Duc et al., 2017; Ngai et al., 2017; Ngai et al., 2020; Tangang et al., 2020; Top et al., 2021). The datasets are downloaded from ESGF index nodes (https://cordex.org/data-access/esfg). The RCP8.5 scenarios within the

fifth Coupled Model Intercomparison Project (CMIP5) are focused due to its more intense rainfall-index projections in comparison to RCP4.5 for the study region (Ngai et al., 2020).

Place Table 1 here

Selection of Rainfall Indices

In this study, we adopt six indicators from the precipitation indices pool suggested by the World Meteorological Organization's Expert Team on Climate Change Detection and Indices (ETCCDI) (Zhang et al., 2011; Cannon et al., 2015). Table 1 gives the details of these indices which can be defined based on annual or seasonal. In this study domain, precipitation basically refers to rainfall. The total precipitation amount (PRCPTOT) is a basic characteristic denoting the amount of rainwater received over the time duration. The maximum daily rainfall (Rx1day), 5-day consecutive rainfall (Rx5day), and 95th percentile of wet-day rainfall amount (R95pTOT) reflect mainly the extreme magnitude of rainfall from different angles. The number of wet days with daily rain amount above 1 mm (R1mm) and 20 mm (R20mm) represent the frequency features of the small and heavy rains. Considering the monsoonal features of both Peninsula Malaysia and Singapore, we use the seasonal data from November to March as northeast monsoon (NEM) and that from May to September as southwest monsoon (SWM).

Place Table 2 here

Method for Bias-Correction and Projection

In this study, the raw RCM outputs will be corrected first using quantile delta mapping (QDM), which has been widely used in bias correction of climatic data. The method was found to be superior than traditional quantile mapping method in mitigating inflation of relative trends in precipitation extreme indices (Cannon et al., 2015). The method could be applied based on monthly, seasonal, or annual data pooled over years depending on the climatic features of the study region. In this study, we adopt the monthly quantile delta mapping (MQDM) as the method for bias correction of daily rainfall time series. In MQDM, the quantile delta mapping is carried out for each month of the year. The corrected monthly data will be eventually aggregated into annual time series. The main step is to find out the relative change, $\delta(t)$, in quantiles between historical benchmark period and projection time point t, which is written as (Cannon et al., 2015):

$$\theta^{s}_{m,proj}(t) = F^{(t,s)}_{m,proj}\left[x^{s}_{m,proj}(t)\right] \quad (1a)$$

$$\delta^{s}(t) = x^{s}_{m,proj}(t)/IF^{s}_{m,hist}\left[\theta^{s}_{m,proj}(t)\right] \quad (1b)$$

where $\theta^{s}_{m,proj}(t)$ is the non-exceedance probability based on model projected rainfall series

180 $x^{s}_{m,proj}(t)$ at time point *t* at month *s* (*s* = 1, 2, …, 12); $F^{(t,s)}_{m,proj}$ is the cumulative distribution
181 function (CDF) constructed based on model projected data over projection window at month *s*
182 covering time point *t*; $IF^{s}_{m,hist}$ is the inverse CDF constructed based on modelled historical data at
183 month *s*.
184
185 Next, the modelled quantile needs to be bias-corrected into historical value using inverse CDF
186 constructed from observed historical data; afterwards, the relative change obtained from the
187 previous step will be multiplied to the historical bias-corrected data to obtain the bias-corrected
188 model projection data. The relevant equations can be written as (Cannon et al., 2015):
189
190 $$cx^{s}_{o,his} = IF^{s}_{o,hist}\left[\theta^{s}_{m,proj}(t)\right] \quad (2a)$$
191 $$cx^{s}_{m,proj} = \delta^{s}(t) \cdot cx^{s}_{o,his} \quad (2b)$$
192
193 where $IF^{s}_{o,hist}$ is the inverse CDF constructed based on observed historical data at month *s*; $cx^{s}_{o,his}$
194 and $cx^{s}_{m,proj}$ are historical bias-corrected model value and bias-corrected model projection value
195 at month *s*, respectively. For more detailed introduction of quantile mapping methods and their
196 comparisons, readers can refer to Cannon et al. (2015) and Tong et al. (2020).
197
198 **3. RESULT ANALYSIS AND DISCUSSIONS**

199 **Evaluation of MQDM Performance**

200 The monthly quantile delta mapping was applied to each RCM rainfall output over the historical

period (1970 to 2005). Figure 2 shows a comparison of observed distribution of rainfall extreme indices based on averaged RCM outputs before and after bias correction at an annual scale. From the observation, the northeast coastal zone seems to have notably higher levels of PRCPTOT, Rx1day, Rx5day, R95pTOT, and R20mm, with most of them representing rainfall magnitude. This is in line with findings from many studies, e.g. Wong et al. (2018) and Khan et al. (2019). The west coast also shows relatively higher values in terms of PRCPTOT and R20mm and the rainy days over 1 mm somewhat spread over most of the peninsula with a range varying from 200 to 260 days. The averaged indices from raw RCM ensembles seem to have significant overestimations over the mountain areas and northeast coast zone, and considerable overestimation over other areas (note the deep red color area in the figure is capped by a maximum limit which is set to avoid over-attenuation of observed values in the same map). The RCMs have seen high estimations over the mountainous areas and northeast coastal areas, possibly due to topographical and monsoonal effects on rainfalls in the model.
The bias-corrected indices are found much closer to the observed ones, with only minor differences detected in certain grids.

Place Figure 2 here

To further verify the performance of quantile mapping over the study domain, a scatter plot

based on all grid data is carried out to compare the modelled result with and without bias correction to the observed one. Figure 3 shows the scatterplots of all indices based on three time scales, including annual, NEM and SWM. The mean absolute errors for raw data (MR) and for bias-corrected data (MQ) averaged over all grids are also shown on each subfigure. It is found that, except for R1mm in NEM, most of the grids have seen overestimation of indices from the raw RCM model. However, all indices in historical runs have been well corrected to observed levels, with MQ values being significantly lower than MR for most indices in various time scales. This has demonstrated the satisfactory capability of MQDM in correcting the raw modelled data in the study region. Comparing to the work of Ngai et al. (2020) for the same region, MQDM seems to have a better correction performance in terms of both annual rainfall and frequency (which is similar to PRCPTOT and R1mm in this study).

Place Figure 3 here

Projection of Future Changes of Indices over the Study Domain

After quantile mapping, the model bias is considered smoothed, and the future varying trends are analyzed in detail. We first investigate the overall distribution of rainfall patterns over the peninsula using 50th percentile of the ensembled RCM outputs, as this could reveal the general trends of rain characteristics in the future by avoiding extreme conditions. Other percentile results (i.e. 25th and 75th) can be found in the Supplementary Materials. Figure 4 shows the

relative changes of annual-based indices under near (2010-2039), middle (2040-2069), and far (2070-2099) future, in comparison to historical benchmark. The result indicates that Rx1day and Rx5day have increment over the entire study domain in all future windows, with later period has a higher increment rate, implying an increased risk of flood for most of the peninsula. At the end of the century, the maximum increment of daily maximum rainfall could reach up to 62.5% and the five-day rainfall could reach up to 43.1% around the inland area. The number of rainy days with amount above 1 mm (R1mm) over the entire peninsula seems to gradually reduce from near to far future, with the largest decrease rate found to be around 14.4% at the end of the century. In terms of annual total rainfall (PRCPTOT), a mixture of both decrease and increase over three future windows is discovered. Interestingly, the west coast, north and south parts would be experiencing a decreasing trend of total rainfall from near (up to -4.7%) to far future (up to -18.4%), while the inland and northeast areas would be experiencing an increasing trend instead (i.e. up to 5.9% and 10.6% in the near and far future, respectively). The R95pTOT is found to generally increase over all future windows (up to 11.3%, 21.5%, and 23.2% in near, middle and far future, respectively), but the north region has seen somewhat decreasing trend in the middle (up to -20.2%) and far future (-22.4%). The R20mm is found increasing over a majority of the peninsula in the future (up to 19.8%, 39.4%, and 41.7% for near, middle and far future, respectively), except for the north and west coast areas which would be experiencing decreasing trend instead (up to -10.2, -42.9, and -42.9% in the near, middle and far future, respectively).

Figures 5 and 6 show the relative changes of rainfall extreme indices based on northeast and

southwest monsoons, respectively. In general, the two monsoons have seen similar increasing trend of Rx1day and Rx5day and decreasing trend of R1mm over most of the areas of the peninsula, which is similar to the annual scale changes. Both monsoons have found wider areas with decreasing trend for PRCPTOT in the middle and far futures. It appears that the northeast coast area would be experiencing a decreasing trend of total rainfall over NEM in the far future while SWM has the opposite result. In terms of P95pTOT, the NEM result is similar to that based on annual scale, where most areas would experience increasing trend except for the north tip of the peninsula. Whereas, the SWM time scale has seen wider areas with decreasing trend along the north, west coast, southwest, and south areas (up to -10.7%, -10.5%, and -10.3% in the near, middle and far future, respectively). The R20mm has mixed increasing and decreasing trends over the peninsula with NEM seen a bit wider range of decrease in the far future while SWM has a wider increase instead.

Place Figures 4-6 here

Analysis of Future Projections based on Climatic Zones

To further quantify the potential changes over different climatic zones of the peninsula Malaysia and Singapore as well as the ensemble uncertainty from multiple RCMs, boxplots are generated for all time scales. Figures 7 to 9 present various indices using their absolute values, where the

286 indices are averaged over the grids within each specific climatic zone (as shown in Figure 1).
287 The bar inside each box denotes the median. The upper and lower box edges represent the 75th
288 and 25th percentiles and the extreme bars above and below denote the maximum and minimum
289 values (whiskers). Outliers are denoted by plus sign and considered abnormal distance values. In
290 the followed zonal analysis, we intend to focus a bit more on higher end values (i.e. upper
291 whiskers) as they represent worst scenarios and have more implications to flood risk in the study
292 domain. In general, the three future windows have shown different levels of uncertainties. The
293 further the future, the wider the result ranges, and vice versa. Also, the deviation of median from
294 the observed value is generally the smallest in the near future, followed by the middle and far
295 future.
296
297 In terms of PRCPTOT, the medians are higher than historical benchmark in NE but are generally
298 lower in NT, SW, IWC and WC. The zones of CT, ST and SE are found to have less significant
299 variations. Taking annual scale in the far future for example, the medians in the far future at
300 zones of CT, IWC, NE, NT, SE, ST, SW, and WC would change by -3.4%, -10.4%, 5.3%, -
301 13.7%, -0.7%, -5.8%, -7.2%, -11.2%, respectively. This is consistent to the results shown from
302 Figures 4 to 6. The ensembled ranges for all zones at all time scales well cover the historical
303 benchmark, suggesting both increase and decrease of PRCPTOT in the future from different
304 models. Under extreme upper conditions (exclude outliers), the relative increase of total rainfall
305 amount in the far future in eight zones could reach up to 21.0%, 13.0%, 32.4%, 30.5%, 41.4%,
306 31.5%, 35.2%, and 22.7% at an annual scale. It is worth noticing that the ensemble range for NE

in the far future is rather wide. The medians at annual, NEM, and SWM are seen only slight changes, namely 5.3%, -2.0%, and 5.7%, respectively. However, the 75th and 25th percentiles would be 20.6% and -15.0% at annual scale, 14.8% and -13.3% at NEM scale, and 30.1% and -15.3% at SWM scale, respectively. Under extreme cases, the total rainfall amount would reach up to 2779.1, 1392.7, 1271.4 mm in NE at annual, NEM, and SWM scales, respectively (corresponding to 32.4%, 38.5%, and 72.6% relative changes with respect to historical benchmark).

In terms of Rx1day, it is basically agreeable by all models that there would be notable increase of maximum daily rainfall in the future at all zones. Taking annual scale in the far future for example, the medians in the far future at zones of CT, IWC, NE, NT, SE, ST, SW, and WC would increase by 52.8%, 50.8%, 37.0%, 26.9%, 42.7%, 34.5%, 33.0%, 44.6%, respectively. Under extreme upper cases (exclude outliers), the index could increase by 169.2%, 164.3%, 101.6%, 106.5%, 56.2%, 87.0%, 80.9%, and 110.8% over eight zones, respectively. In terms of monsoonal results, NEM seems to be more consistent with annual scale, implying a more dominant effect of NEM in maximum daily rainfall. Taking far future for example, the extreme relative increases for NEM are 107.9%, 89.3%, 84.8%, 108.5%, 45.5%, 85.4%, 71.0%, and 66.1% over eight zones, respectively; those for SWM are 78.8%, 58.6%, 79.6%, 50.0%, 95.4%, 45.0%, 43.4%, and 39.5%, respectively. In addition, the NEM have seen a larger spatial variation of Rx1day and also a wider ensemble range than SWM, implying stronger effect of northeast wind from South China sea.

328

329 Figure 8 shows the boxplots for Rx5day and R95pTOT. Similar to the changes of Rx1day, there
330 is obvious increment of 5-day consecutive rainfall over all zones based on both annual and
331 monsoonal scales. Taking far future at annual scale for example, the medians of Rx5day would
332 increase by 30.6%, 35.3%, 16.7%, 12.6%, 22.6%, 37.1%, 27.2%, 25.0% at zones of CT, IWC,
333 NE, NT, SE, ST, SW, and WC, respectively; under extreme cases, the increase would be
334 112.8%, 109.6%, 57.0%, 103.9%, 30.5%, 52.0%, 59.5%, and 86.9%, respectively. NEM has
335 seem a closer pattern of changes to the annual scale in terms of ensemble range and spatial
336 variations in comparison to SWM. Taking far future at NE as an example, it is suggested from
337 model 75th percentile that the Rx5day would be 255.3, 232.8, and 111.6 mm at annual, NEM,
338 and SWM scales, respectively; at 25th percentile, it becomes 164.4, 155.6, ad 79.8 mm,
339 respectively; under extreme cases, it could reach up to 282.2, 268.4, 131.5 mm, respectively.
340

341 The varying trend of R95pTOT is somewhat similar to that of Rx5day, except for a lesser degree
342 of increment in comparison to historical benchmark. The medians of R95pTOT at annual scale in
343 the far future would change by 12.8%, 3.9%, 18.8%, -14.1%, 7.4%, 5.0%, 4.8%, -1.4% at zones
344 of CT, IWC, NE, NT, SE, ST, SW, and WC, respectively; under extreme upper cases, the
345 changes (exclude outliers) would become 62.4%, 46.0%, 52.0%, 66.3%, 17.2%, 24.3%, 24.0%,
346 and 48.3%, respectively. The index at the NE zone would still have the widest fluctuation and
347 also the highest extremes in the far future. The maximum R95pTOT (exclude outliers) at annual,
348 NEM, and SWM scales would reach up to 751.1, 382.0, and 207.3 mm (which correspond to

relative changes of 52.0%, 53.7%, and 56.7%), respectively. The index at SWM scale does not seem to have a clear cut of increase or decrease in most zones, as the medians are relatively close to the historical benchmark values; while the index at NEM scale seems to have the 25th percentile closer to historical benchmark, implying a higher possibility of increment.

Figure 9 presents the boxplots of R1mm and R20mm. It is found that the frequency of rainy days (>1 mm) would drop significantly over all zones under various future windows. The ensemble range, similar to other indices, would become wider from near to far future. The medians of R1mm at annual scale in the far future would drop by -7.0%, -7.1%, -7.4%, -8.9%, -6.5%, -3.6%, -6.1%, -7.4% at zones of CT, IWC, NE, NT, SE, ST, SW, and WC, respectively; under extreme lower cases, the decrease (exclude outliers) would be as low as -10.9%, -19.0%, -17.6%, -23.6%, -9.4%, -9.4%, -20.2%, and -21.9%, respectively. The zone NT has seen the most notable decrease of R1mm, where the 75th and 25th percentiles would be 226 and 196 days at annual scale, 68 and 61 days at NEM scale, and 108 and 101 days at SWM, respectively. Under extreme cases (exclude outliers), the R1mm would reduce to as low as 181, 50, and 75 days at annual, NEM, and SWM scales (which correspond to -23.6%, -32.4%, and -34.2%), respectively; the west coastal area (WC) is also seen a notable decrease of R1mm in the far future, namely -21.9, -30.0, and -27.4% at annual, NEM and SWM scales, respectively.

The R20mm have seen a mixed increase and decrease at all zones. In terms of medians, the R20mm at annual scale in the far future would change by 5.7%, -0.6%, 10.5%, -28.0%, 10.1%, -

11.1%, 11.8%, and -25.2%, respectively; under extreme upper case, R20mm would increase by 71.0%, 44.2%, 67.7%, 89.2%, 88.5%, 54.9%, 166.7%, and 79.3%, respectively. It is found that the medians at NEM scale in different zones are close to the historical benchmarks, while those at SWM scales are clearly below benchmarks in IWC, NT, ST, and WC, above benchmarks in NE and SE, and close to benchmarks in CT and SW. The ensemble ranges at NE in the far future seem to be the widest among all. The medians at annual, NEM and SWM are 22, 13, and 6 days, respectively; those under extreme cases, the index could rise up to 34, 21, and 16 days or become as low as 14, 9, and 2 days, respectively.

Place Figures 7-9 here

Generally, the rainfall indices based on various RCM model outputs have indicated long-term variations both temporally and spatially. From near to far future, the variations of indices would increase with greater level of uncertainties. From the overall peninsula, most model imply more intense rainfall extremes (like Rx1day, Rx5day, and R95pTOT) in the future, implying higher possibility of flooding risk. For instance, the relative increments of the medians from RCM models averaged over all climatic zones in the far future are 40.3%, 25.9%, and 4.7% for Rx1day, Rx5day and R95pTOT, respectively. The annual rainfall amount (PRCPTOT) in the long run would likely increase mainly in the northeast coastal zone and drop in most of other

areas over the peninsula, with the median being -5.9% averaged over all zones. The frequency of wet days (R1mm) would generally drop over the whole peninsula, with the median averaged over all zones being -6.8% in the far future. The frequency of heavy rains (R20mm) would overall decrease (by -3.4% in average in the far future) but might still notably increase in the northeast zone (NE) at both annual and southwest monsoon. The extreme condition implied from various RCM models would be more alarming. Moreover, the rainfall characteristics in northeast coastal zone has been found to be relatively more sensitive to climate change, as it may be more affected by monsoonal effects. Finally, the spatial variability at NEM is found somewhat closer or more consistent to that at annual scale than SWM, particularly for those extreme indices like Rx1day, Rx5day, R95pTOT, and R20mm, implying a more dominant role of NEM in extreme rainfall distribution over the year.

Further Discussions

This study took the full advantage of the CORDEX-SEA precipitation dataset and revealed the future rainfall characteristics over the region of Malay Peninsula and Singapore. The study followed the works of Ngai et al. (2020) and Supari et al. (2020) by focusing on the Peninsula Malaysia and Singapore region based on six standard ETCCDI precipitation extreme indices over near, middle and far future windows. A direct comparison to these previous work is difficult due to selection of different indices, bias-correction method, future windows, and RCM scenarios. However, a partial comparison is still possible for general trend detection. From quantile mapping, Ngai et al. (2020) revealed an overall overestimation of annual rainfall

412 (similar to PRCTTOT), FREQ (roughly to R1mm) and Q90 (roughly similar to R95pTOT) in
413 terms of ensemble average of seven RCM models in the historical period from 1986 to 2005.
414 This is somewhat similar to our study findings. It is also found that the MQDM method used in
415 this study performs generally better than the QM method in Ngai et al. (2020), at least in terms of
416 annual rainfall, frequency of rainy days, and upper percentile of wet days. For future predictions,
417 Ngai et al. (2020) found out that FREQ is generally decreasing over the western Malaysia in both
418 middle and far future, which is consistent with what we concluded from this study. Ngai et al.
419 (2020) also indicated that the Q90 would be decreasing in most of the peninsula, except for the
420 northeast and south zones. Our findings indicate a decreasing trend of R95pTOT mainly in the
421 north, west coastal, and south zones, with larger areas having increasing trends. From the work
422 of Supari et al. (2020), it was revealed that the PRCPTOT under RCP8.5 of eight RCMs have
423 suggested about 10-20% decrease over the entire western Malaysia at the end of this century and
424 about 1-20% increase for Rx1day. This is somewhat consistent to our general study results for
425 these two indicators except for some local variations like northeast coastal zone for PRCPTOT.
426
427 Nonetheless, our study has also given a more holistic view of the ensemble ranges of the six
428 indices in different future windows, and also more focused examination of changes over different
429 climatic zones over the study domain. The study result would be a good addition to the academic
430 community for revealing the essential spatiotemporal variations of rainfall over the southern
431 Malay peninsula from short- to long-term futures and supporting large-scale flood risk
432 assessment and adaptation planning. Secondly, the study framework can be easily followed by

many other countries, especially developing countries, to explore updated information of climate patterns and rainfall trends in the future. The relevant datasets (like APHRIDIATE and CORDEX) are easily assessable and would be useful for regional studies with limited data sources.

This study is based on ensembled rainfall data from nine RCM outputs and APHRODITE, where the grid data may not be able to catch higher spatial resolution rainfall patterns. But the quantile mapping approach is also applicable to gauge-based data or other higher-resolution grid rainfall products if they are available. Moreover, to facilitate flood risk management, higher temporal resolution rainfall is desired. The sub-daily CORDEX datasets (like 3-hourly) are also available in many regions around the world. It is possible to carry out quantile mapping on sub-daily rainfall data but such efforts may be restricted by the availability of historical sub-daily data for the study region and also the justification of the methodology's validity in bias-correct sub-daily data which is not widely tested. Lastly, the monthly quantile delta mapping method is proved to be rather reliable in correcting the six indices that are linked to rainfall amount, extremes, and frequency. However, the reliability of the method in reproducing other more complicated indices, like dry/wet spell lengths, frequencies of rainfall extremes etc., may need further testing.

4. CONCLUSIONS

452 This study explored future variations of rainfall characteristics over peninsula Malaysia and
453 Singapore region based on rainfall indices of PRCPTOT, Rx1day, Rx5day, R95pTOT, R1mm,
454 and R20mm, under 9 CORDEX-SEA RCM datasets with RCP8.5 emission scenario. A monthly
455 quantile delta mapping method (MQDM) was adopted for bias-correction of the RCM modelled
456 data. It was revealed that the adopted quantile mapping method is satisfactory in correcting the
457 modeled rainfall data for the historical record. From future projection, it was indicated that all
458 the studied rainfall indices have long-term variations both temporally and spatially. Generally,
459 the further the future, the higher the variability and uncertainty of indices. For the study region,
460 Rx1day, Rx5day, and R95pTOT have obvious increment over the whole peninsula. The annual
461 rainfall amount (PRCPTOT) in the long run would likely increase mainly in the northeast coastal
462 zone and drop in most of other areas. The frequency of wet days (R1mm) would generally drop
463 over the whole peninsula and that of heavy rains (R20mm) would overall decrease in average in
464 the far future but might still notably increase in the northeast zone (NE).
465
466 The study result would be useful in revealing the essential spatiotemporal variations of rainfall
467 over the peninsula from short- to long-term futures and supporting large-scale flood risk
468 assessment and adaptation planning. Also, the method framework can be easily followed by
469 many other countries, especially developing countries, to explore updated information of climate
470 patterns and rainfall trends in the future. In further studies, it would be valuable to explore sub-
471 daily quantile mapping methods due to availability of sub-daily rainfall data from CORDEX.
472 Also, further testing of MQDM in correcting other more complicated indices are necessary.

ACKNOWLEDGEMENT

This study was supported by AcRF Tier 1 project (2019-T1-001-160) from Ministry of Education (MOE), Singapore. We acknowledge the data support from APHRODITE (http://aphrodite.st.hirosaki-u.ac.jp/) and the Southeast Asia Regional Climate Downscaling (SEACLID)/Coordinated Regional Climate Downscaling Experiment for Southeast Asia (CORDEX-SEA) project (which was funded by ARCP2014-07CMY-Tangang and ARCP2015-04CMY-Tangang). We thank the World Climate Research Programme's Working Groups on both Regional Climate and Coupled Modelling, as well as other climate modelling groups (listed in Table 2 of this paper) for producing and making available their model output. We also acknowledge the Earth System Grid Federation infrastructure an international effort led by the U.S. Department of Energy's Program for Climate Model Diagnosis and Intercomparison, the European Network for Earth System Modelling and other partners in the Global Organisation for Earth System Science Portals (GO-ESSP).

Data Availability Statement: The data used to support the findings of this study are available from the corresponding author upon request.

Conflict of Interest: The authors declare that they have no conflict of interest.

Funding Statement: This study was supported by AcRF Tier 1 project (2019-T1-001-160) from Ministry of Education (MOE), Singapore.

Author's Contribution: Dr. Xiaosheng Qin: writing - original draft, conceptualization, methodology, formal analysis, data curation, visualization; Dr. Dai Chao: review & editing, validation; Mr. Liu Lilingjun: review & editing, data curation.

Code Availability: The code used to support the findings of this study are available from the corresponding author upon request.

Ethics Approval: For this type of study formal consent is not required.

Consent to participate: Not Applicable.

Consent for publication: The authors are affirming that all necessary consents have been obtained for this work.

REFERENCES

Ahmad, F., Ushiyama, T., Sayama, T. (2017). Determination of Z-R relationship and inundation analysis for Kuantan River Basin, Research Publication No. 2/2017, Malaysian Meteorological Department (MMD), Ministry of Science, Technology and Innovation (MOSTI), published by Jabatan Meteorologi Malaysia Jalan Sultan.

Amin, M., Shaaban, A.J., Ercan, A. et al. (2017). Future climate change impact assessment of watershed scale hydrologic processes in Peninsular Malaysia by a regional climate model coupled with a physically-based hydrology modelo., Science of the Total Environment, 575: 12–22.

Bronaugh, D., 2014: climdex.pcic: PCIC implementation of Climdex routines. Pacific Climate Impacts Consortium, R package version 1.1-1.

Cannon, A. J., Sobie, S. R., & Murdock, T. Q. (2015). Bias Correction of GCM Precipitation by Quantile Mapping: How Well Do Methods Preserve Changes in Quantiles and Extremes?, Journal of Climate, 28(17), 6938-6959.

Cavendish Square Publishing, World and Its Peoples: Eastern and Southern Asia. Marshall Cavendish Reference. 2007. New York. ISBN 978-0-7614-7631-3.

Chow, W.T.L. (2017) The impact of weather extremes on urban resilience to hydro-climate hazards: a Singapore case study. International Journal of Water Resources Development, 34(4): 510-524.

Donat, M.G., Sillmann, J., Wild, S., Alexander, L.V., Lippmann, T., Zwiers, F.W. (2014) Consistency of temperature and precipitation extremes across various global gridded in sity and reanalysis datasets. Journal of Climate, 27: 5019-5035.

525 Evans, J.P. (2011). CORDEX – An international climate downscaling initiative, the 19th
526 International Congress on Modelling and Simulation, Perth, Australia, 12–16 December 2011.
527 Giorgi, F., Jones, C., Asrar, G.R., 2009. Addressing climate information needs at the regional level:
528 the CORDEX frame-work. WMO Bull. 58 (3), 175–183.
529 Giorgi F, Coppola E, Solmon F, Mariotti L and others (2012) RegCM4: model description and
530 preliminary tests over multiple CORDEX domains. Clim Res 52:7-29.
531 Hai, O.S., Samah, A.A., Chenoli, S.N., Subramaniam, K., and Mazuki, M.Y.A. (2017) Extreme
532 rainstorms that caused devastating flooding across the east coast of Peninsular Malaysia during
533 November and December 2014. Weather and Forecasting, 32: 849-872.
534 Li, X., Zhang, K., Babovic, V. (2019). Projections of future climate change in Singapore based on
535 a multi-site multivariate downscaling approach, Water, 11, 2300:1-22.
536 Kjellström, E., Bärring, L., Nikulin, G., Nilsson C., Persson, G., Strandberg, G. (2016) Production
537 and use of regional climate model projections – A Swedish perspective on building climate
538 services. Clim. Ser. 2-3: 15-29.
539 Khan, N., Pour, S.H., Shahid, S., Ismail, T., Ahmed, K., Chung, E.S., Nawaz, N., and Wang, X.
540 (2019). Spatial distribution of secular trends in rainfall indices of Peninsular Malaysia in the
541 presence of long-term persistence, Meteorological Applications, 26: 655-670.
542 Ngai, S.T., Tangang, F., Juneng, L., 2017. Bias correction of global and regional simulated daily
543 precipitation and surface mean temperature over Southeast Asia using quantile mapping method.
544 Glob. Planet. Chang. 149, 79–90.
545 Ngai, S.T., Sasaki, H., Murata, A., Nosaka, M., Chung, J.X., Juneng, L., Supari, E., Supari,
546 Salimun, E., and Tangang, F. (2020a). Extreme rainfall projections for Malaysia at the end of

21st century using the high resolution Non-Hydrostatic Regional Climate Model (NHRCM), SOLA, 16: 132-139.

Ngai, S.T., Juneng, L., Tangang, F., Chung, J.X., Salimun, E., Tan, M.L., Amalia, S. (2020b) Future projections of Malaysia daily precipitation characteristics using bias correction technique, Atmospheric Research 240: 104926.

Ngo-Duc, T., et al., 2017. Performance Evaluation of RegCM4 in Simulating Extreme Rainfall and Temperature Indices over the CORDEX-Southeast Asia Region. 37. pp. 1634–1647.

Richard, S., Walsh, K.J.E. (2018) The influence of El Niño–Southern Oscillation on boreal winter rainfall over Peninsular Malaysia, 134: 121-138.

Suhaila, J., Deni, S.M., Zin, W.Z.W., Jemain, A.A. (2010). Trends in Peninsula Malaysia rainfall data during the southwest monsoon and northeast monsoon seasons: 1975-2004, Sains Malaysiana, 39(4): 533-542.

Tan, M.L., Juneng, L., Tangang, F.T., Samat, N., Chan, N.W., Yusop, Z., Ngai, S.T. (2020), SouthEast Asia HydrO-meteorological droughT (SEA-HOT) framework: A case study in the Kelantan River Basin, Malaysia, Atmospheric Research, 246: 105155.

Tangang, F., Farzanmanesh, R., Mirzaei, A., Supari, Salimun, E., Jamaluddin, A.F., and Juneng, L. (2017) Characteristics of precipitation extremes in Malaysia associated with El Niño and La Niña events, International Journal of Climatology, 37: 696-716.

Tangang, F., Santisirisomboon, J., Juneng, L. et al. (2019). Projected future changes in mean precipitation over Thailand based on multi-model regional climate simulations of CORDEX Southeast Asia, International Journal of Climatology, 39(14): 5413-5436.

Tangang, F., Chung, J.X., Juneng, L. et al. (2020) Projected future changes in rainfall in Southeast

569 Asia based on CORDEX–SEA multi-model simulations. Clim Dyn 55, 1247–1267.
570 Tong, Y., Gao, X.J., Han, Z.Y., Xu, Y.Q., Xu, Y., Giorgi, F. (2020). Bias correction of temperature
571 and precipitation over China for RCM simulations using the QM and QDM methods, Climate
572 Dynamics, https://doi.org/10.1007/s00382-020-05447-4.
573 Sun, Q., Miao, C., Duan, Q., Ashouri, H., Sorooshian, S., and Hsu, K.L. (2017) A review of global
574 precipitation data sets: data sources, estimation, and intercomparisons. Review of Geophysics,
575 56: 79-107.
576 Top S, Kotova L, Cruz LD, Aniskevich S and others (2021) Evaluation of regional climate models
577 ALARO-0 and REMO2015 at 0.22° resolution over the CORDEX Central Asia domain.
578 Geoscientific Model Development, 14(3), 2021: 1267–1293,
579 Wong, C.L., Liew, J., Yusop, Z., Ismail, T., Venneker, R., and Uhlenbrook, S. (2016) Rainfall
580 characteristics and regionalization in Peninsular Malaysia based on a high resolution gridded
581 data set, Water, 8, 500: 1-16.
582 Wong, C.L., Yusop, Z., Ismail, T. (2018) Trend of daily rainfall and temperature in Peninsular
583 Malaysia based on gridded data set, International Journal of GEOMATE, 14(44): 65-72.
584 Yatagai, A., K. Kamiguchi, O. Arakawa, A. Hamada, N. Yasutomi and A. Kitoh, 2012:
585 APHRODITE: constracting a long-term daukt gridded precipitation dataset for Asia based on a
586 dense network of rain gauges, Bull Amer Meteorol Soc 93(9): 1401-1415.
587 Zhang, X., L. Alexander, G. C. Hegerl, P. Jones, A. Klein Tank, T. C. Peterson, B. Trewin, and F.
588 W. Zwiers (2011) Indices for monitoring changes in extremes based on daily temperature and
589 precipitation data. Wiley Interdiscip. Rev.: Climate Change, 2, 851–870.

Table Captions:

Table 1. Selected RCMs with scenario RCP8.5 from CORDEX-SEA database

Table 2. Precipitation extreme indices used in this study

Table 1. Selected RCMs with scenario RCP8.5 from CORDEX-SEA database

No.	RCM (Develop Institute)	GCM (Develop Institute)	Responsible Institutes (Country)	Example References for RCMs
1	RegCM4-7 (ICTP, Italy)	HadGEM2-ES (MOHC, UK)	ICTP (Italy)	Giorgi et al. (2012)
2	REMO2015 (GERICS, Germany)	MPI-ESM-LR (MPI-M, Germany)	GERICS (Germany)	Top et al. (2021)
3	RCA4 (SMHI, Sweden)	CNRM-CM5 (CNRM-CERFACS, France)	SMHI (Sweden)	Kjellström et al. (2014); Tangang et al. (2020)
4	RegCM4-7 (ICTP, Italy)	NorESM1-M (NCC, Norway)	ICTP (Italy)	Giorgi et al. (2012)
5	RegCM4-3 (ICTP, Italy)	MPI-ESM-MR (MPI-M, Germany)	RU-CORE (Thailand)	Tangang et al. (2020)
6	RegCM4-3 (ICTP, Italy)	IPSL-CM5A-LR (IPSL, France)	RU-CORE (Thailand)	Tangang et al. (2020)
7	RegCM4-3 (ICTP, Italy)	GFDL-ESM2M (NOAA, USA)	RU-CORE (Thailand)	Tangang et al. (2020)
8	RCA4 (SMHI, Sweden)	HadGEM2-ES (MOHC, UK)	SMHI (Sweden)	Kjellström et al. (2014); Tangang et al. (2020)
9	RegCM4-3 (ICTP, Italy)	EC-EARTH (EC-Earth consortium)	RU-CORE (Thailand)	Tangang et al. (2020)

* Sources: https://cordex.org/data-access/esgf/; https://cordex.org/domains/region-14-south-east-asia-sea/

Table 2. Precipitation extreme indices used in this study

Abbreviation*	Description (defined over annual or seasonal scale)	Unit
PRCPTOT	Total precipitation amount	mm
Rx1day	Maximum daily rainfall amount	mm
Rx5day	Maximum consecutive 5-day precipitation amount	mm
R95pTOT	Total precipitation amount from wet days with precipitation amount above 95th percentile	mm
R1mm	Number of days with precipitation amount above (inclusive) 1 mm	days
R20mm	Number of days with precipitation amount above (inclusive) 20 mm	days

* Sources: Bronaugh et al. (2014) and Cannon et al. (2015)

Figure Captions:

Figure 1. Study map and climatic zones following Wong et al. (2016).

Figure 2. Distribution of annual-based historical indices of (a) PRCPTOT, (b) Rx1day, (c) Rx5day, (d) R95pTOT, (e) R1mm, and (f) R20mm from (1) observed data, (2) averaged RCM data, and (3) averaged RCM bias-corrected data.

Figure 3. Scatterplot of historical indices of (a) PRCPTOT, (b) Rx1day, (c) Rx5day, (d) R95pTOT, (e) R1mm, and (f) R20mm based on averaged RCM outputs before and after QM under time scales of (1) annual, (2) NEM, and (3) SWM. Note: MR and MQ are the averaged MAEs for raw and bias-corrected data over all grids, respectively.

Figure 4. Relative changes of annual-based (a) PRCPTOT, (b) Rx1day, (c) Rx5day, (d) R95pTOT, (e) R1mm, and (f) R20mm under (1) near (N), (2) middle (M), and (3) far (F) future windows compared to baseline based on 50th percentile of the ensembled RCM outputs.

Figure 5. Relative changes of NEM-based results based on similar settings as Figure 4.

Figure 6. Relative changes of SWM-based results based on similar settings as Figure 4.

Figure 7. Projection of changes of (1) PRCPTOT and (2) Rx1day with time scales at (a) annual, (b) NEM, and (c) SWM under various RCM results. Note: horizontal dashed line represents observed historical benchmark; N, M, and F represent near, middle and far future.

Figure 8. Projection of changes of (1) Rx5day and (2) R95pTOT with time scales at (a) annual, (b) NEM, and (c) SWM under various RCM results. Note: symbols have similar meanings as those in Figure 7.

Figure 9. Projection of changes of (1) R1mm and (2) R20mm with time scales at (a) annual, (b) NEM, and (c) SWM under various RCM results. Note: symbols have similar meanings as those in Figure 7.

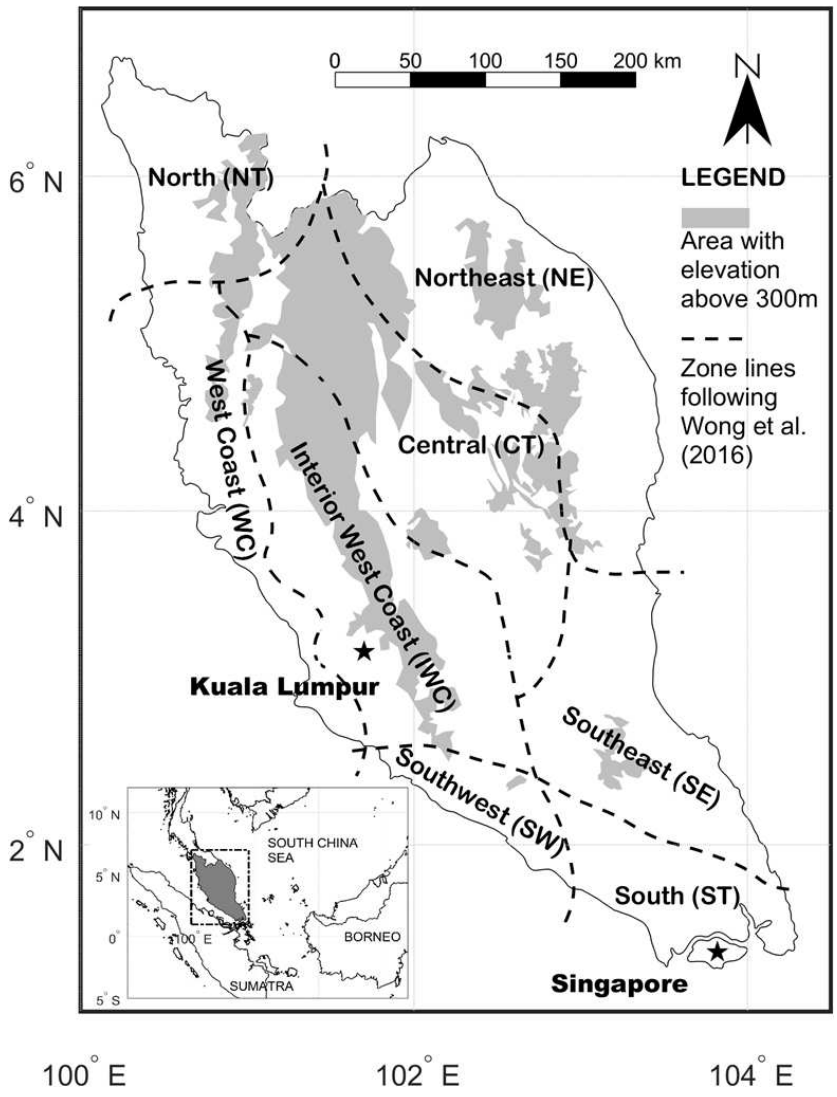

Figure 1. Study map and climatic zones following Wong et al. (2016).

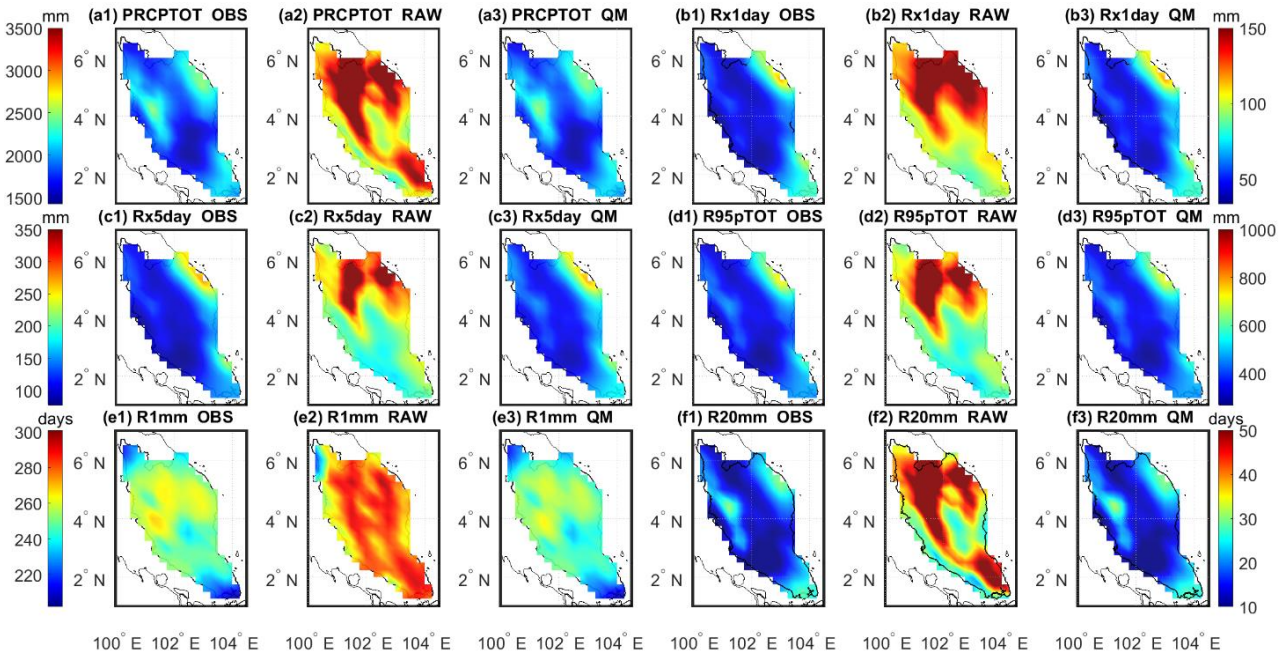

Figure 2. Distribution of annual-based historical indices of (a) PRCPTOT, (b) Rx1day, (c) Rx5day, (d) R95pTOT, (e) R1mm, and (f) R20mm from (1) observed data, (2) averaged RCM raw data, and (3) averaged RCM bias-corrected data.

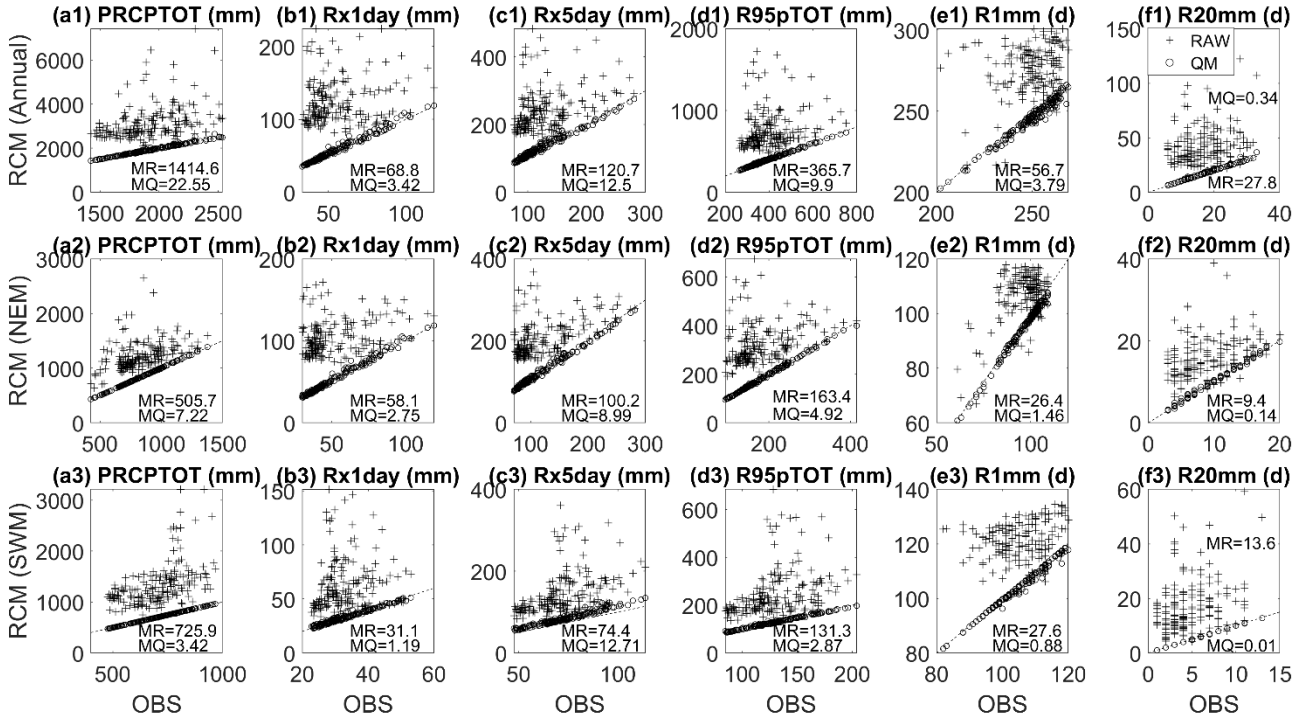

Figure 3. Scatterplot of historical indices of (a) PRCPTOT, (b) Rx1day, (c) Rx5day, (d) R95pTOT, (e) R1mm, and (f) R20mm based on averaged RCM outputs before and after QM under time scales of (1) annual, (2) NEM, and (3) SWM. Note: MR and MQ are the averaged MAEs for raw and bias-corrected data over all grids, respectively.

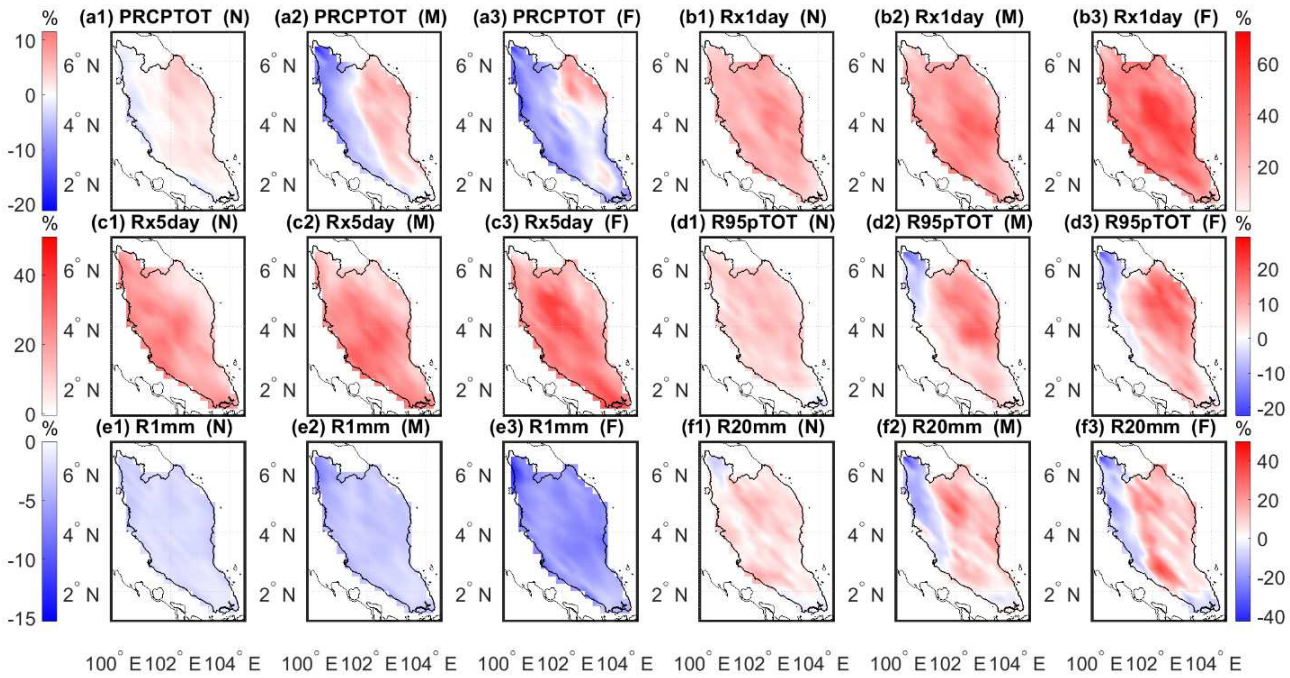

Figure 4. Relative changes of annual-based (a) PRCPTOT, (b) Rx1day, (c) Rx5day, (d) R95pTOT, (e) R1mm, and (f) R20mm under (1) near (N), (2) middle (M), and (3) far (F) future windows compared to baseline based on 50th percentile of the ensembled RCM outputs.

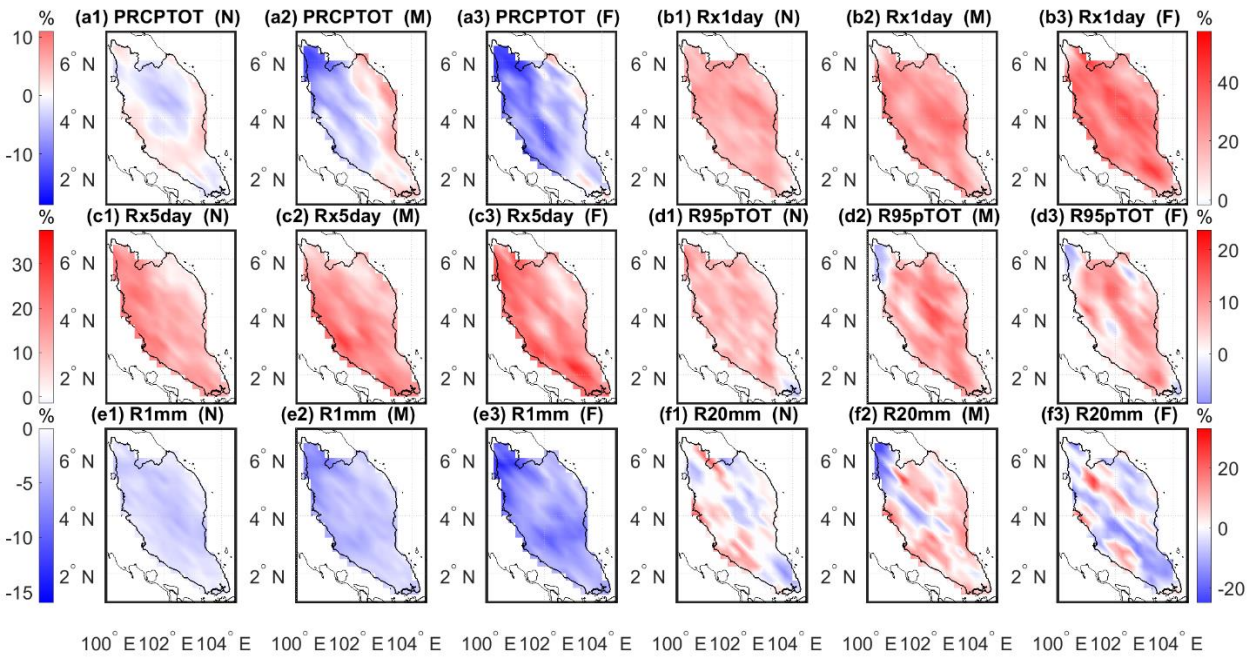

Figure 5. Relative changes of NEM-based results based on similar settings as Figure 4.

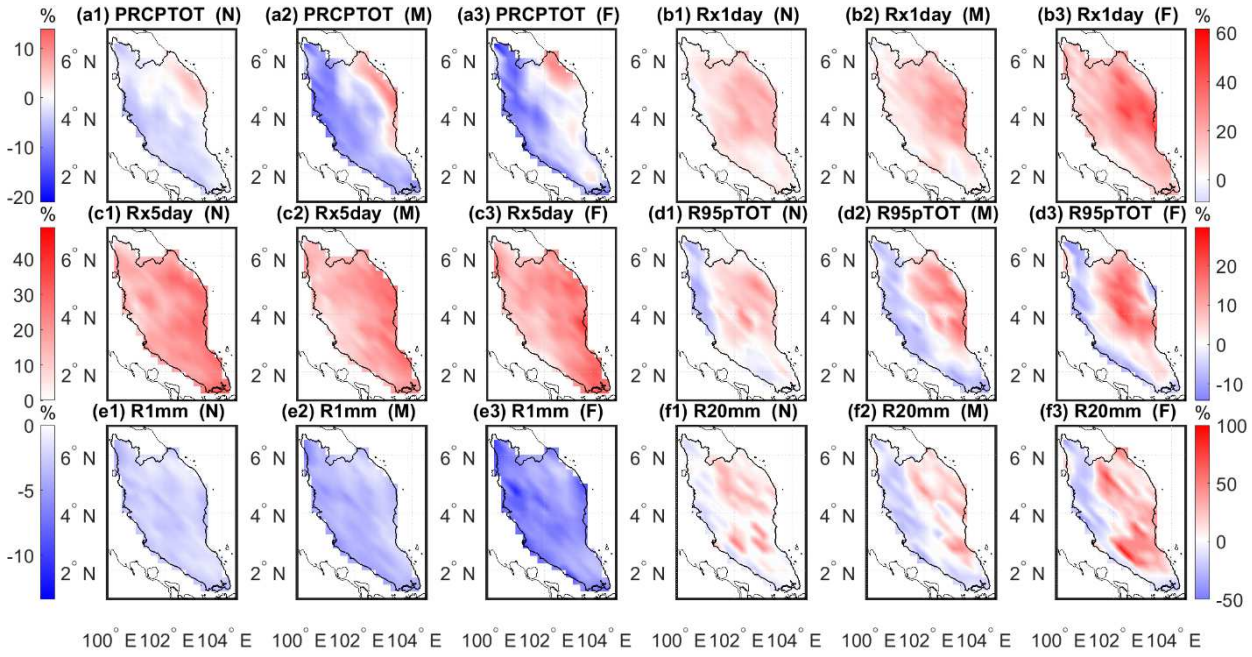

Figure 6. Relative changes of SWM-based results based on similar settings as Figure 4.

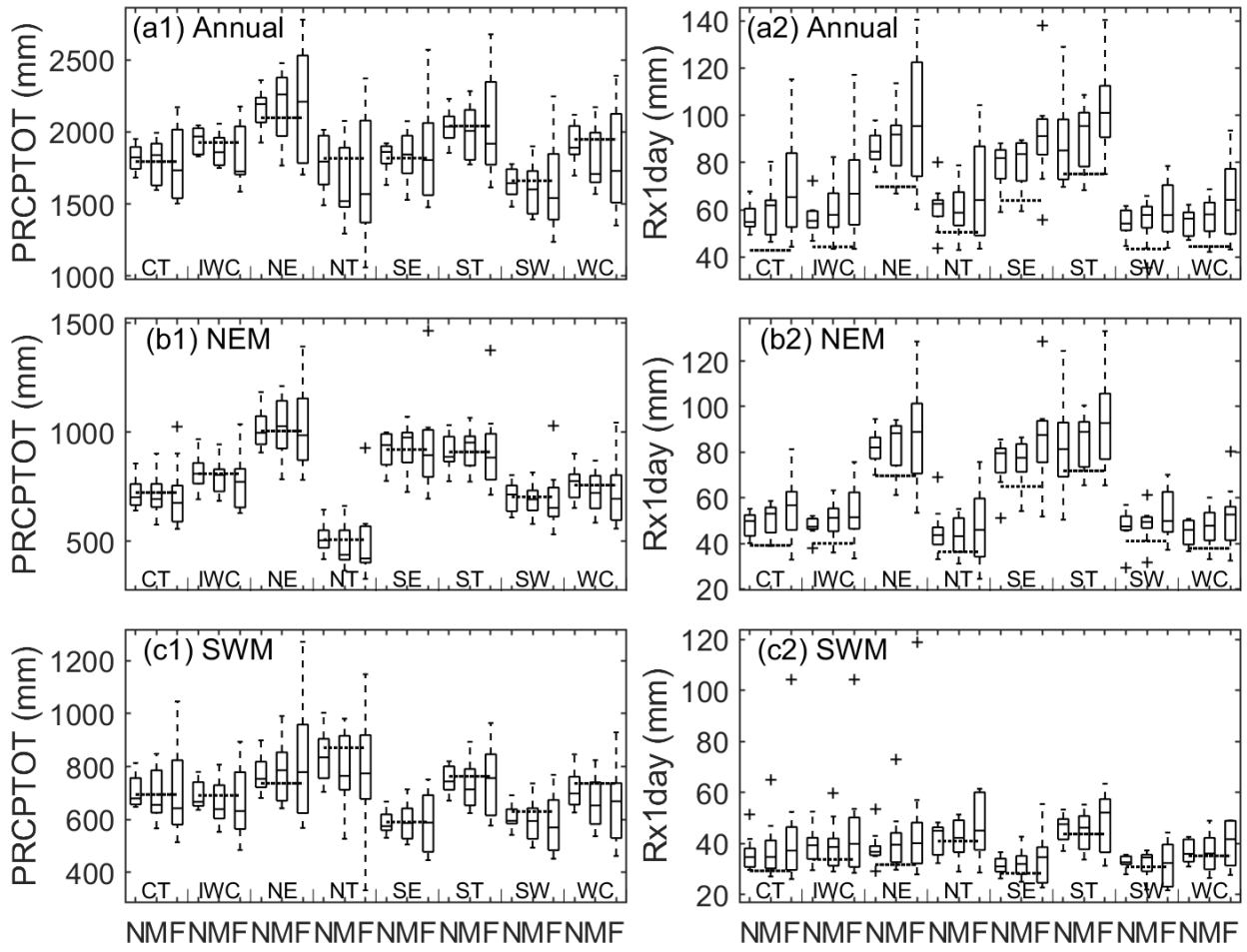

Figure 7. Projection of changes of (1) PRCPTOT and (2) Rx1day with time scales at (a) annual, (b) NEM, and (c) SWM under various RCM results. Note: horizontal dashed line represents observed historical benchmark; N, M, and F represent near, middle and far future.

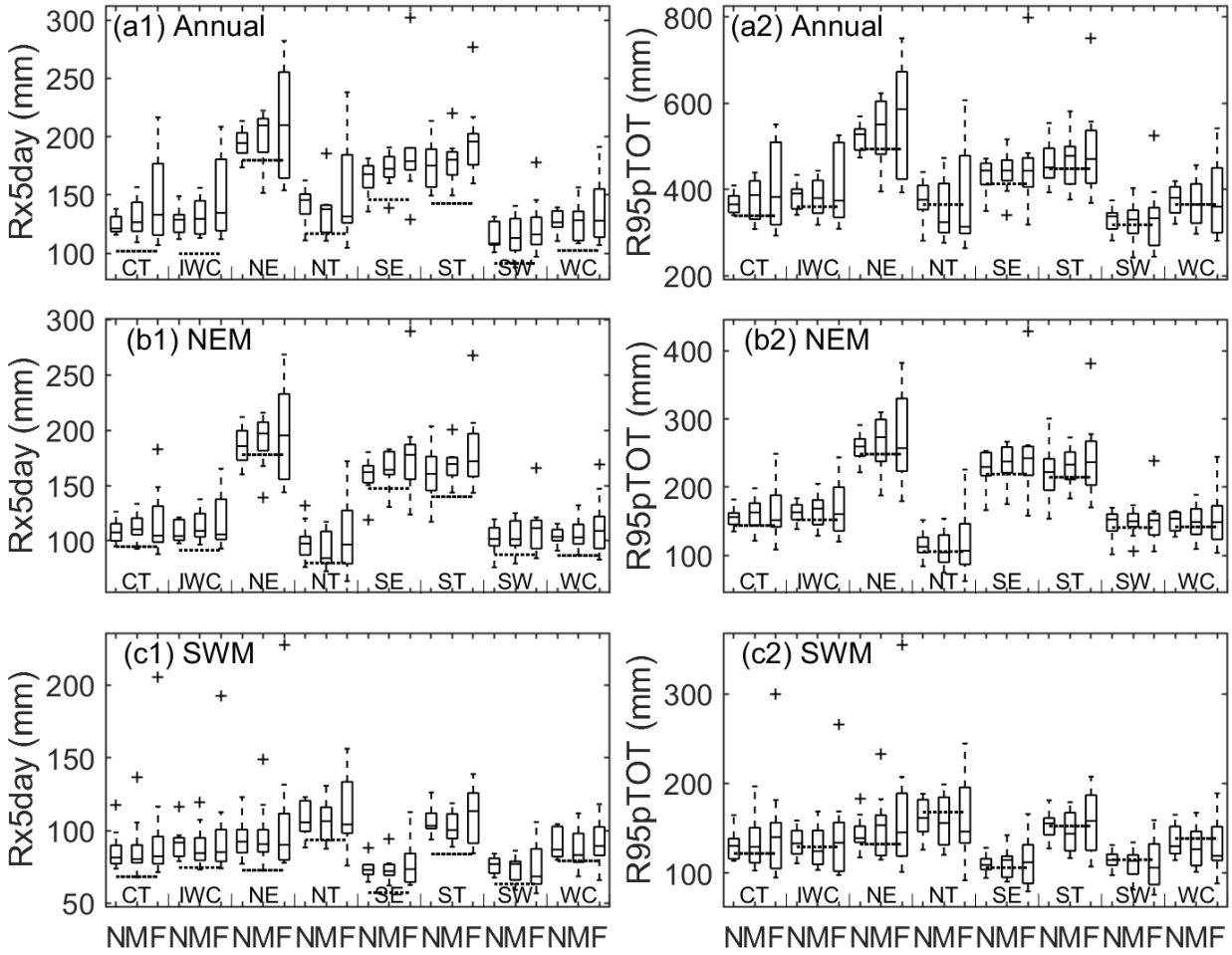

Figure 8. Projection of changes of (1) Rx5day and (2) R95pTOT with time scales at (a) annual, (b) NEM, and (c) SWM under various RCM results. Note: symbols have similar meanings as those in Figure 7.

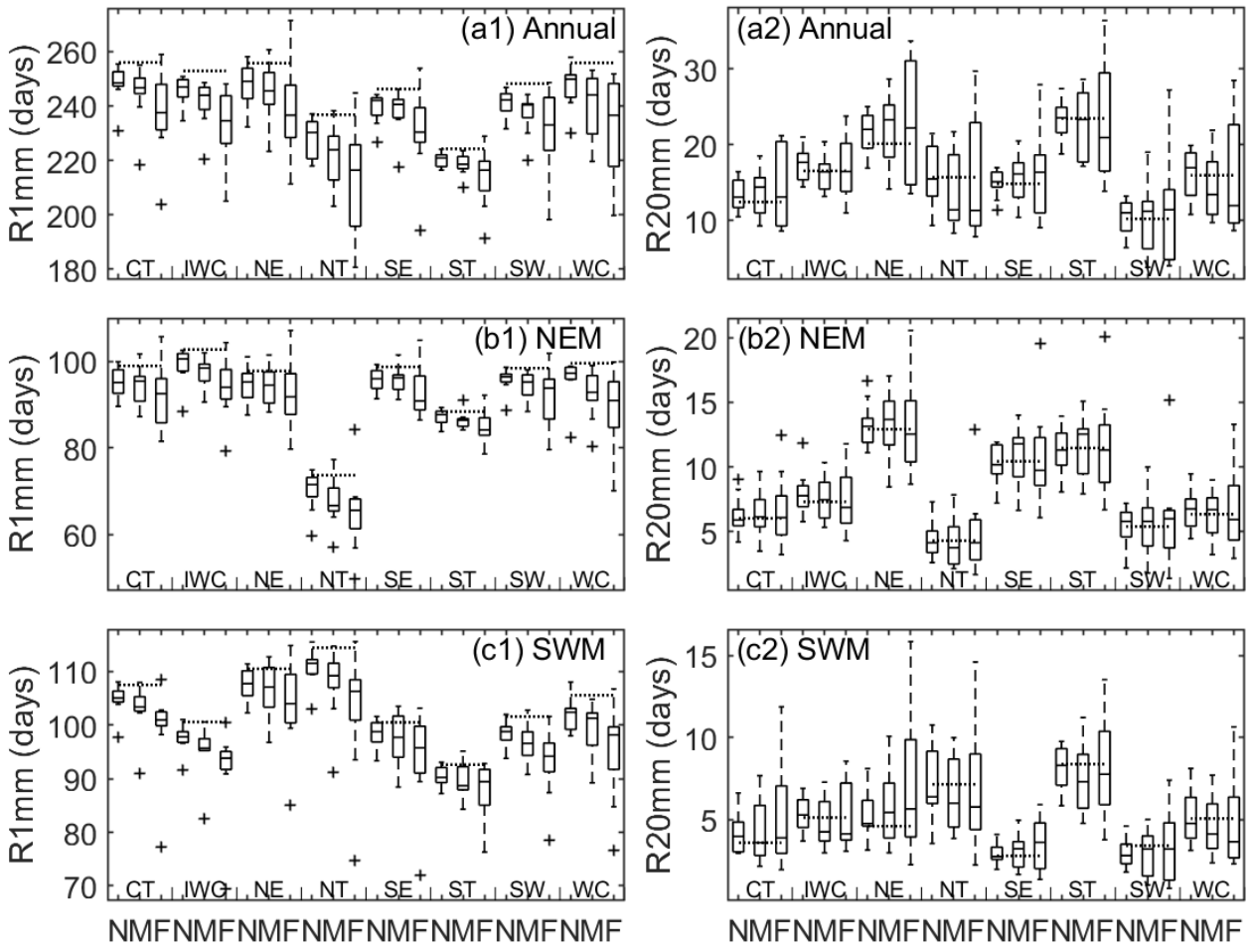

Figure 9. Projection of changes of (1) R1mm and (2) R20mm with time scales at (a) annual, (b) NEM, and (c) SWM under various RCM results. Note: symbols have similar meanings as those in Figure 7.

Supplementary Files

This is a list of supplementary files associated with this preprint. Click to download.

- SupplementaryDocuments.docx